Scanning Microscopy

Volume 1995
Number 9 *Luminescence*

Article 1

1995

Cathodoluminescent Properties of Single Crystal Materials for Electron Microscopy

Rudolf Autrata
Academy of Sciences of the Czech Republic

Petr Schauer
Academy of Sciences of the Czech Republic, petr@isibrno.cz

Scanning Microscopy Supplement 9, 1995 (Pages 1-12) 0892-953X/95$5.00+.25
Scanning Microscopy International, Chicago (AMF O'Hare), IL 60666 USA

CATHODOLUMINESCENT PROPERTIES OF SINGLE CRYSTAL MATERIALS FOR ELECTRON MICROSCOPY

Rudolf Autrata and Petr Schauer*

Institute of Scientific Instruments, Academy of Sciences of the Czech Republic,
Brno, Czech Republic

Abstract

The results of measurements of cathodoluminescence efficiencies, decay characteristics and emission spectra of YAG:Ce, YAP:Ce, P47 (Y_2SiO_5:Ce) and CaF_2:Eu single crystals at excitation by electrons with an energy of 10 keV and a current density of the order of 10^{-8} A·cm^{-2} are presented. Advantages and disadvantages of the individual single crystals intended for application in electron microscopes are dealt with. Attention is paid to the photomultiplier tube (PMT) matching, degradation and afterglow of the mentioned single crystals. For YAG:Ce, the effect of the activator concentration of crystals and the effect of the cleaning and annealing of crystal plates are included. The proposal for the application of YAG:Ce as a scintillator and as an image screen in electron microscopy is given. Sizes of electron interaction areas and absorbed energy distributions are simulated by using Monte Carlo method based on the plural large angle elastic scattering. Cathodoluminescence widths of YAG:Ce single crystals for an impact electron in the energy range 10-100 keV are estimated.

Key Words: Cathodoluminescence, single crystals, scintillation detectors, imaging screens, electron microscopes, efficiency, decay time, emission spectrum, photomultiplier tube (PMT) matching, Monte Carlo.

*Address for correspondence:
Petr Schauer
Academy of Sciences of the Czech Republic,
Institute of Scientific Instruments,
Kralovopolska 147,
CZ-612 64 Brno,
Czech Republic

Telephone number: (42 5) 41321246
FAX number: (42 5) 41211168
E-mail: petr@isibrno.cz

Introduction

Owing to their electron beam radiation damage resistance and some other properties discussed in the paper, single crystal materials are becoming an element which is more and more frequently used in imaging systems in electron microscopes (EM). Single crystal cathodoluminescent (CL) materials are employed not only in scanning EM (SEM) and scanning transmission EM (STEM) scintillation detectors, for which they were originally developed (Autrata *et al.*, 1978, 1983), but also as CL screens both for direct observation {usually by means of a light optical microscope, as described by Delong *et al.* (1994)}, and for indirect observation when the image is transmitted to the television (TV) screen using a charge-coupled device (CCD) camera (Batson, 1988; Krivanek *et al.*, 1991; Arii *et al.*, 1993). To ensure a maximum usefulness of CL single crystals in all these applications, all their basic CL properties must be considered. These include: (1) CL efficiency (more precisely: energy conversion efficiency), (2) time characteristics (decay time), and (3) spectral emission characteristics. The enumerated properties are little dependent on the energy of entering signal electrons, if single crystals are homogeneous. For the screen resolution, the size of electron and photon interaction volumes (which are, on the contrary, strongly dependent on the energy of signal electrons) is important. Last but not the least, optical properties of single crystals are of importance in EM applications. They play a decisive role in collection of the optical signal (Schauer and Autrata, 1992a).

Experimental

At our laboratory, some tens of different single crystal CL materials were measured. Of these, single crystals of cerium activated yttrium aluminum garnet (YAG:Ce - $Y_3Al_5O_{12}:Ce^{3+}$), cerium activated yttrium aluminum perovskite (YAP:Ce - $YAlO_3:Ce^{3+}$), cerium activated yttrium silicate ($Y_2SiO_5:Ce^{3+}$, which chemically corresponds to the powder phosphor P47), and europium activated calcium fluoride ($CaF_2:Eu^{2+}$) were

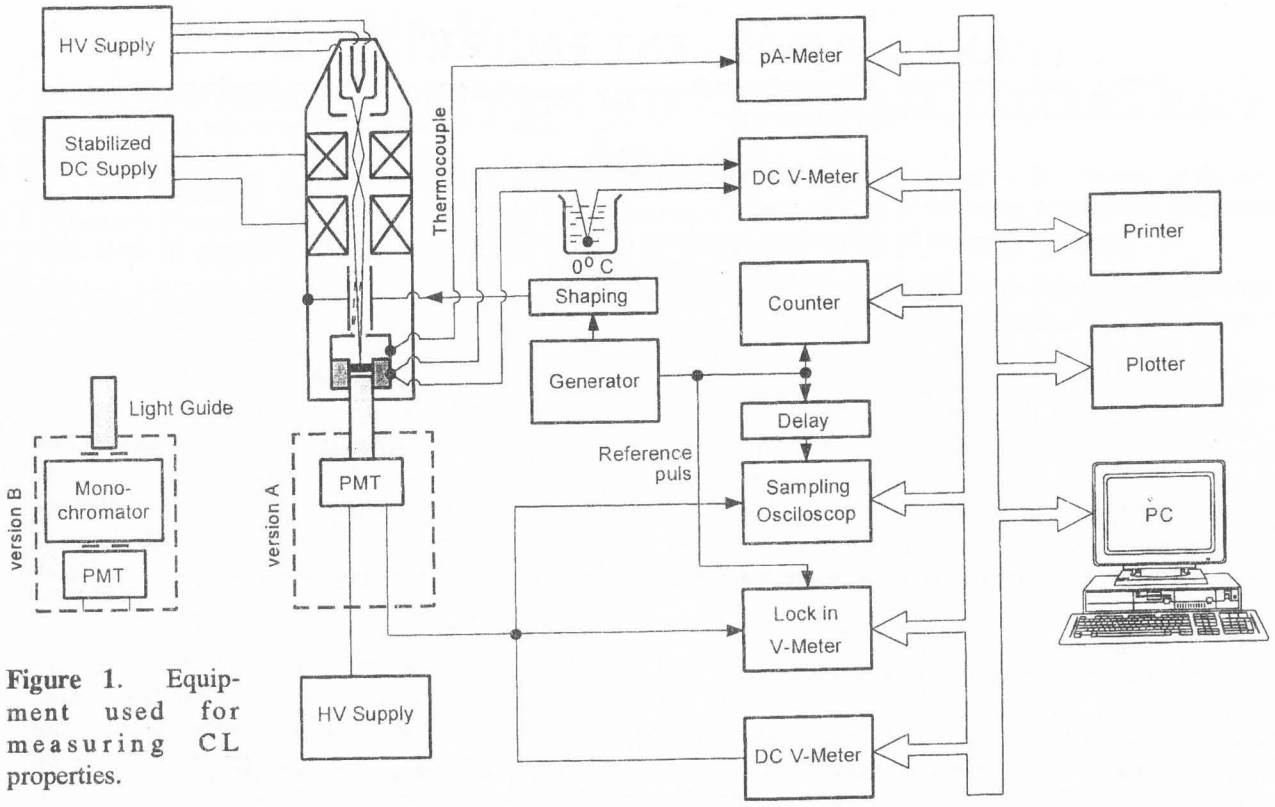

Figure 1. Equipment used for measuring CL properties.

chosen as the most interesting ones for EM applications. The single crystals were pulled by Czochralski method using molybdenum crucibles, resistance heating and 98% Ar + 2% H_2 protective atmosphere. The initial material contained less than 10^{-4} wt% of impurities (Kvapil *et al.*, 1981, 1988).

The as grown single crystals were cut and ground into the form of discs 10 mm in diameter and 0.5 mm thick. The surface intended for the output of photons was matted so that the relief roughness was approximately 0.2 μm. The surface intended for the input of electrons was polished. All specimens were cleaned in organic solvents, some specimens were additionally cleaned by boiling them in acids. Some specimens were annealed in an oxidizing or a reducing atmosphere, O_2 and H_2 respectively, at a temperature of 1500-1700°C. For all specimens, the side intended for the input of electrons was coated with a thin aluminum film (50 nm) to prevent the charging of the surface on the one hand, and to increase the light signal collection efficiency (Schauer and Autrata, 1992b) on the other hand.

The CL properties were measured by using an equipment built in our laboratory (Fig. 1). The excitation unit was formed by an adapted desk-top electron microscope Tesla BS242 with an electrostatic deflection system and a blanking diaphragm placed above the Faraday cage. In the pulse mode, the excitation electron beam could be then deflected outside the blanking diaphragm. In our work, electrons with an energy of 10 keV were used for the excitation. For these electrons, the rise and decay times of the excitation pulse were approximately 5 ns each. The pulse mode was intended, above all, for the determination of kinetic properties, but it was also used with advantage for the measurement of emission spectra. The CL efficiency was measured in the continuous mode.

The investigated single crystal specimen was positioned at the face of the light guide (inside the Faraday cage). Using this light guide, the signal was guided directly toward the entrance window of the photomultiplier tube (PMT), when spectrally non-decomposed CL properties (integral efficiency and decay characteristics) were measured. For measurement of spectrally decomposed CL properties (spectral characteristics), the signal was guided toward the entrance slit of the mirror monochromator. For the former variant, the Tesla 65 PK 415 PMT (S20 photocathode) with a very fast but low efficiency circular focused multiplication system was used. During the measurement of efficiency and decay characteristics, the output of this PMT was connected to the micro-voltmeter and the sampling oscilloscope, respectively. For the latter variant of the signal light-guiding, a slower but high efficiency EMI 9558B PMT (S20 photocathode) was positioned at the output slit of the mirror monochromator. The signal from the output of EMI PMT was measured using a lock-in nanovoltmeter.

Table 1. Spectral properties of single crystals for EM.

Single Crystal	spectral characteristic			
	maximum[1] (nm)	FWHM[2] (nm)	S20 PMT matching[3] (%)	S11 PMT matching[4] (%)
YAG:Ce	560	122	73	45
YAP:Ce	366	52	60	58
P47	420	77	85	80
CaF_2:Eu	426	30	92	88

[1]Position of the maximum of the main emission band. [2]Full width of the half maximum of the main emission band [3,4]Matching to the spectral response of [3]S20 and of [4]S11 photocathode.

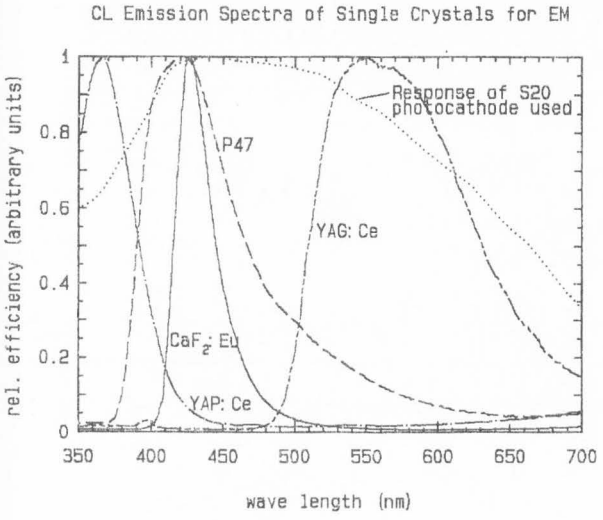

Figure 2. Normalized CL spectra of single crystals for EM.

The individual instruments were connected to the Hewlett Packard interface bus (HPIB), and the measuring apparatus was controlled by a personal computer which also processed the obtained data. The data measuring and processing software which contains correction algorithms and provides output data in the form of tables and graphics was written in programming languages Turbo Pascal and Basic.

Survey of CL Properties of Single Crystals for EM

The CL emission spectrum, CL efficiency (emission intensity), and decay time are three basic CL properties which are important not only for the estimation of suitability of the single crystals application in EM but also for the physical analysis of cathodoluminescence.

The CL emission spectra of YAG:Ce, YAP:Ce, P47 and CaF_2:Eu single crystals together with the spectral sensitivity of the S20 photocathode used are shown in Figure 2. Each emission spectrum is corrected for spectral sensitivity of the PMT used and normalized with regard to its maximum value. This gives better information about the position of the emission bands but at the same time makes the comparison of intensities impossible. For each single crystal, the position of the maximum of the emission band and the value of the full width at half maximum (FWHM) together with the value of the spectral matching to the S20 photocathode used, as well as to S11, are given in Table 1. It follows from the results summarized in the table that the CaF_2:Eu and YAP:Ce single crystals show the best and the worse spectral matching, respectively, to the S20 PMT used. However, the spectral matching of YAP:Ce could be markedly increased by using the PMT with the quartz entrance window. It is not the photocathode itself but the glass entrance window that causes the low spectral sensitivity of PMT in the short wave spectrum region.

The YAG:Ce is the only single crystal that is suitable for CL screens for direct observation. Unlike other investigated single crystals, it emits light in the yellow spectrum region, and this is very favorable for the human eye. On the contrary, this is unfavorable for conventional PMTs with alkali photocathodes. In the case of YAG:Ce, it is necessary to use the S20 photocathode (its long wave spectrum region differs from that of S11). All other single crystals investigated can also work with the S11 photocathode. In addition to the characteristic broad yellow emission band with a maximum at 560 nm, the YAG:Ce shows a very weak emission in the blue, violet and UV spectrum regions. This weak emission which is more marked for specimens with a low activator concentration (see, Fig. 3) has a sharp maximum at 400 nm which is superimposed on the broad emission band with a maximum in the UV region, i.e., beyond the capabilities of the measuring device used.

Table 2. Efficiency of single crystals for EM.

Single Crystal	relative efficiency[1]			forming[5]
	corrected[2] for PMT	as measured[3] (S20 PMT)	estimated[4] (S11 PMT)	after 3 hours (%)
YAG:Ce	100	73	45	2.8
YAP:Ce	142	85	82	1.2
P47	126	107	101	0.8
CaF_2:Eu	131	120	115	2.4

[1]Related to the corrected value of YAG:Ce. [2]Corrected for the spectral response of the S20 photocathode used.
[3]Uncorrected for the spectral response of the S20 photocathode used; measured 30 minutes after the start of excitation.
[4]Estimated if the S11 photocathode were used. [5]Efficiency decreasing during given time (related to the initial value).

Table 3. Decay properties of single crystals for EM.

Single Crystal	time characteristic		
	decay time[1] (ns)	corrected decay time[2] (ns)	afterglow[3] (%)
YAG:Ce	110	103	2.0
YAP:Ce	45	38	0.5
P47	41	34	unmeasurable
CaF_2:Eu	1200	1200	1.3

[1]uncorrected and [2]corrected for the time response of the measuring equipment.
[3]intensity measured 5 μs after the end of excitation.

For all applications in EM, high CL efficiency is required. The relative CL efficiency of the investigated single crystals is shown in Table 2. The values of this quantity are always related to the corrected value of YAG:Ce single crystal. The as measured integral (spectrally non-decomposed) efficiency includes the influence of the PMT photocathode spectral sensitivity. This quantity is interesting from the viewpoint of application in scintillation detectors where the effects of the PMT photocathode cannot be avoided. In contrast to this, the efficiency corrected for the spectral sensitivity of the S 20 photocathode used is interesting from the physical point of view, and it allows estimation of changes expected in connection with an application of some other photocathode, as shown in column 4 of Table 2.

For all single crystal CL materials, the degradation of efficiency was very low. For electrons with an energy of 10 keV and a current density of 4 x 10^{-8} A·cm^{-2}, the forming of the efficiency of all single crystal measured was observed. This was represented by the efficiency decreasing less than 3% during the first three hours, as is evident from the last column of Table 2.

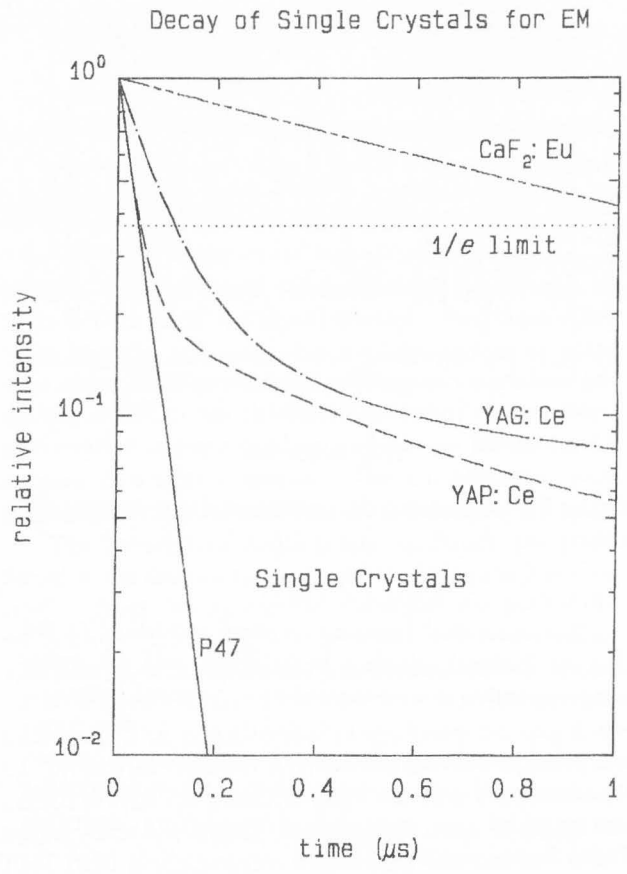

Figure 3. Decay characteristics of single crystals for EM. Excitation pulse duration 10 μs.

Table 4. Cerium concentration data and activator and defect CL intensities of YAG:Ce single crystals investigated.

crystal Number	weight content CeO_2 (g)	weight content $Y_3Al_5O_{12}$ (g)	cerium concentration in melt (mol%)[1]	cerium concentration in crystal[2] (mol%)[1]	distribution coefficient	relative intensity[3] (%) activator em. at 560 nm	relative intensity[3] (%) defect em. at 360 nm
1313	0.03	550	6.3×10^{-3}	1.3×10^{-3}	0.21	5.3	0.115
1303	0.5	400	1.4×10^{-1}	2.9×10^{-2}	0.21	31	0.112
1310	3.0	400	8.6×10^{-1}	1.3×10^{-1}	0.15	72	0.056
1320	7.0	400	2.0	3.2×10^{-1}	0.16	100	0.047

[1]Number of cerium atoms per 100 yttrium atoms. [2]Measured using activation neutron analysis.

[3]Related to the intensity of the activator emission of the crystal number 1320.

The efficiency decrease was only temporal to a great extent. So, when the measurement was repeated later, similar results, but within a shorter time period, were obtained, and no additional degradation took place.

Typical CL decay characteristics for YAG:Ce, YAP:Ce, P47 and CaF_2:Eu single crystals are shown in Figure 3. The values of the decay time and afterglow are resulted in Table 3. The typical excitation pulse duration was 10 μs. Both yttrium aluminate single crystals (YAG:Ce and YAP:Ce) have multi-exponential decay characteristics. On the other hand, P47 and CaF_2:Eu single crystals have single exponential decay curves, with measured decay times of 41 ns and 1.2 μs, respectively. The measured decay time of YAG:Ce is 110 ns and the afterglow (measured 5 μs after the end of excitation) amounts to 2%. For YAP:Ce, the measured decay time is only 45 ns and the afterglow amounts to less than 1%. In fact, with respect to the fall time of the pulse of the excitation electron beam (5 ns) and the fall time of PMT (2 ns), the short-term decay component must be corrected by subtracting approximately 7 ns of the fall time of the measuring equipment. The short-term component of the CL decay of both yttrium aluminate single crystals depends only negligibly on the duration of excitation. On the contrary, the long-term component of the CL decay depends strongly on the duration of excitation, so that for a very short excitation the afterglow of YAG:Ce and YAP:Ce can be one order and at least two orders lower, respectively. This is advantageous for applications in SEM/STEM electron detectors operating at the TV rate, because the images with a rich topographic content can be of higher quality.

Unfortunately, all single crystals that have their CL decay time shorter than 100 ns (which is the condition when the TV scan frequency is used) contain oxygen and just this group of single crystals belongs to those with the least efficiency (Robbins, 1980; Dorenbos *et al.*, 1992; Lempicki, 1993). This means that calcium fluoride, which is the most efficient of the four chosen, has only limited applicability because its decay time constant is 1.2 μs. The greatest advantage of YAP:Ce single crystals and P47 is that they are the fastest (38 ns and 34 ns, respectively). Especially, they have no such a marked component of long persistent luminescence as the YAG:Ce single crystals have. The only disadvantage of YAG:Ce single crystals is their speed which can be behind the limit for the TV rate in some cases. It is therefore necessary to search for a way to shorten the decay time of YAG:Ce scintillators.

YAG:Ce Single Crystals

The YAG:Ce single crystal suggests the widest applicability in EM. It is very popular, although its decay time is more than two times longer than that of the YAP:Ce, and its energy conversion efficiency is only 2/3 to 3/4 of that of the YAP:Ce single crystal or P47. The reason for this is, that (1) it is technologically the most easily attainable (and thus the cheapest), (2) unlike the other chosen single crystals, it has its CL emission maximum in the yellow region of the spectrum (and is thus suitable also for direct observation), (3) its decay time (100 ns) is still sufficient for the TV scan frequency, and (4) its optical self-absorption is low (therefore, it is applicable in bulk geometry).

Activator concentration effect

For the measurement of the activator concentration influence on the CL properties of YAG:Ce single crystals, a set of four crystals was used. The weight contents of their initial materials together with the determined concentration and the distribution coefficient are summarized in Table 4. The plates under investigation were cut from the middle part of the crystals, a pair of plates from each crystal. Of these, one plate was used for the measurement of the CL properties and the other

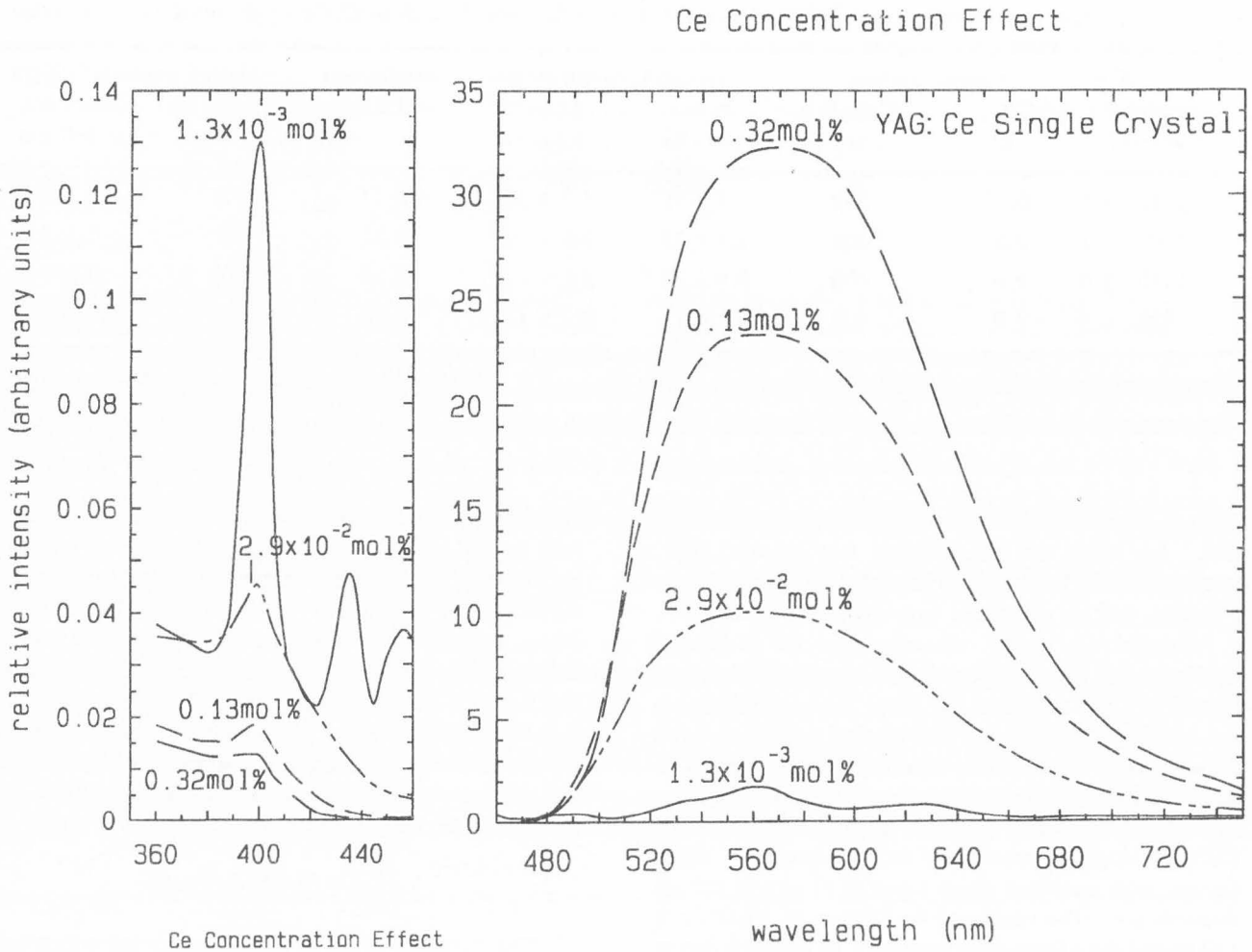

Figure 4. Influence of the activator concentration of the YAG:Ce single crystal on the CL emission spectrum and on the CL intensity.

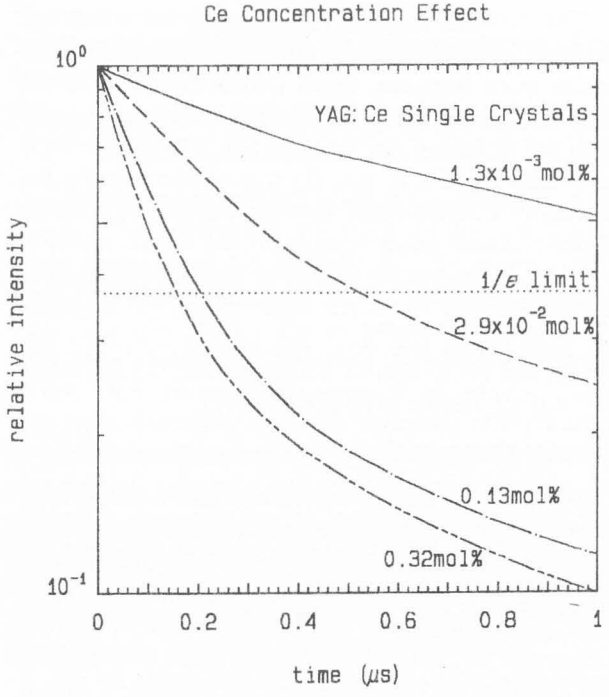

Figure 5. Influence of the activator concentration of the YAG:Ce single crystal on the decay of CL intensity.

for the neutron activation analysis. The results presented do not hold for the whole volume of the grown crystal, because in the initial stage of the growth the crystal has more defects, is less homogeneous and has as many as 2.5 times lower concentration of cerium ions. It is evident from Table 4 that the distribution coefficient is lower for higher concentrations of the activator.

Figure 4 shows the emission spectra of all specimens whose activator concentrations are given in Table 4. The obtained curves hold for the as-grown (unannealed) single crystal plates cleaned not only by using ethyl alcohol but also by boiling them in aqua regia (see next chapter). To make the arrangement of the results shown in Figure 4 more clear, for the 350-460 nm spectral region, a vertical scale different from that of the remaining part of the spectrum was used. The spectral characteristics of specimens of different concentrations are not normalized, so that intensities of the individual

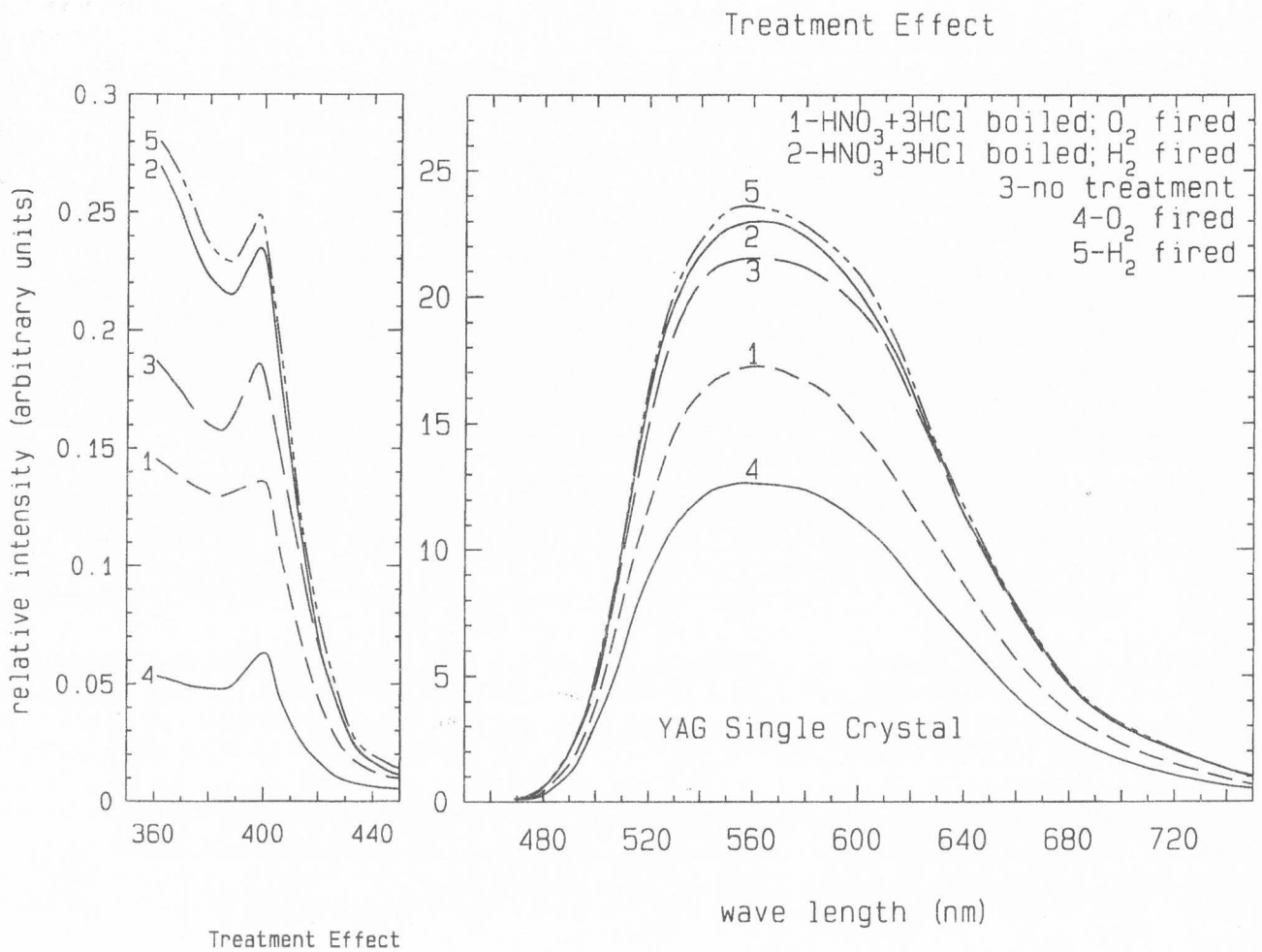

Figure 6. Effect of cleaning and annealing of YAG:Ce single crystal on emission spectrum and intensity.

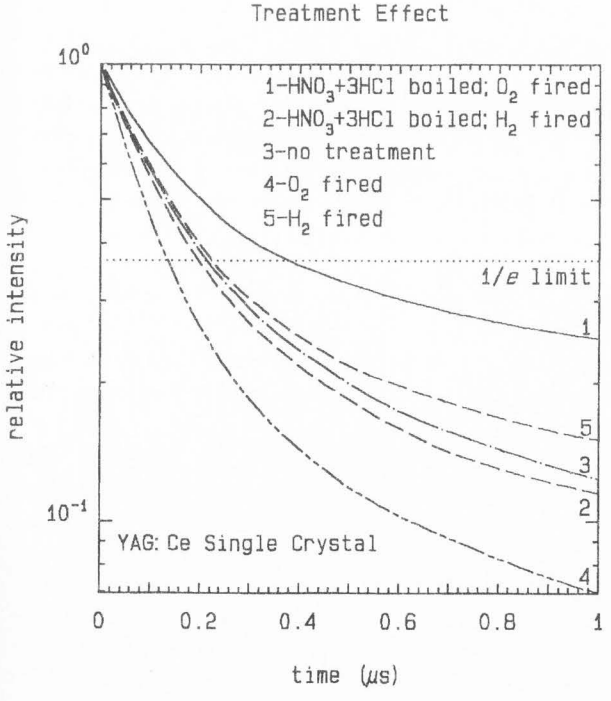

Figure 7. Influence of the cleaning and annealing of the YAG:Ce single crystal on the decay of CL.

---

emission bands shown in Figure 4 can be compared even with the results presented in the next chapter. The relative intensities of activator and defect emissions are included in Table 4, too.

The emission band with a maximum at 560 nm represents the characteristic emission from the activator (Robbins *et al.*, 1979). The position of this emission band practically does not change with changing Ce concentration but its intensity I increases with increasing concentration C ($I \approx C^{0.6}$) up to 10^{-1} mol% of cerium in the crystal. Behind this limit, a deviation from the dependence begins to manifest itself. Using extrapolation, it can be estimated that the concentration quenching probably starts from an activator concentration of about 1-2 mol%. Unfortunately, it was not possible to grow a YAG:Ce single crystal with a Ce concentration higher than 0.32 mol% because for a Ce concentration in the melt higher than 2 mol% there was a sharp decrease in the magnitude of the distribution coefficient. If one

succeeded in growing a single crystal with a higher activator concentration, a slight increase in the efficiency of the characteristic CL could be expected.

It can be seen from Figure 4 that all YAG:Ce specimens have a broad emission band with a maximum in the UV region. This is a case of defect emission (Robbins *et al.*, 1979) whose intensity also depends on the activator concentration, but unlike the characteristic emission it is nearly constant (see, Table 4) up to a Ce concentration in the crystal of about 3×10^{-2} mol%. Then it decreases with increasing activator concentration. From the viewpoint of quality, the emission spectra of specimens with the least concentration are very similar to the spectra of an undoped YAG single crystal. For these specimens with the least Ce concentration, all maxima are distinct, as are those for YAG:Nd. The results of measurement of both the characteristic and the UV emission are rather inaccurate for the 1.3×10^{-3} mol% Ce concentration. On one hand, it is difficult to determine such a low activator concentration, and, on the other hand, to judge whether the emission under measurement is or is not influenced by the presence of other nominally undoped impurities. In the initial raw materials, the nominally undoped impurities can be contained in comparable concentrations.

The results of measurement of the CL decay of YAG:Ce single crystals with different activator concentrations are shown in Figure 5. The measurement of the decay of spectrally undecomposed intensity was made using the series of specimens described in Table 4. The course of characteristics considerably depends on the activator concentration in the crystal. The specimens with the highest attainable Ce concentration (0.32 mol%) have the shortest decay time (156 ns). On the contrary, for the YAG:Ce specimens with a very low Ce concentration (1.3×10^{-3} mol%), the decay time is more than one order higher (2 μS). However, the emission spectra of the latter specimens suggest (see, Fig. 4) that unlike specimens with higher concentrations, the obtained result cannot unambiguously be ascribed to the emission from the activator (560 nm). The YAG:Ce decay characteristic can be described using the multi-exponential function of type $I = \Sigma A_i \cdot \exp(t/\tau_i)$, where I is the intensity at the time t, and A_i and τ_i are the intensity coefficient and the decay time constant of the i-th decay component, respectively. When the activator concentration is decreased, the long time decay components begin to manifest themselves more markedly at the cost of the component with the shortest decay constant.

Cleaning and annealing effect

Cutting, grinding and polishing of single crystals using special agents imply quite a drastic intervention in the surface layer of the specimens. It will be later described more in detail that when luminescence is excited by using electrons with an energy of 10 keV, the most important processes take place at a depth smaller than 1 μm, i.e., in the surface layer, where mechanical effects of abrasive and polishing agents can cause not only a damage of the crystalline structure but they can also introduce impurities into it.

Figures 6 and 7 show emission spectra and decay characteristics of YAG:Ce single crystals (0.13 mol% Ce) cleaned or annealed in different ways. It is obvious from Figure 6 that the way of specimen treatment does not influence the position of the emission bands. Substantial changes can be seen only in the emission intensity in different spectral regions. Curve 3 represents measurement of an unannealed specimen that was cleaned in organic solvents and coated with a thin aluminum layer. No other treatments were used. Specimen 5 was cleaned the same way as specimen 3 and annealed in a reducing atmosphere (H_2) at a temperature of 1500°C for a period of 5 hours. For this specimen, the emission intensity increased very markedly in the UV spectral region. A similar effect has been found for specimen 2 that was additionally cleaned by boiling in aqua regia and annealed in the reducing atmosphere under the same conditions as specimen 5. When the specimen was cleaned the same way as specimen 3 and annealed in a oxidizing atmosphere (O_2) at a temperature of 1500°C for a period of 5 hours, a considerable decrease in emission took place, particularly in the UV region, as shown by curve 4. Curve 1 proves that the influence of the oxidizing atmosphere on the emission intensity is limited when the specimens are cleaned by boiling in aqua regia prior to their annealing. This way of treatment causes a uniform decrease in the intensity in the whole spectrum region measured. This means that the specimens annealed in the reducing atmosphere have the highest efficiency whereas the specimens annealed in the oxidizing atmosphere have the least efficiency. The plates which were additionally cleaned by boiling in aqua regia have mostly a higher efficiency than those cleaned only in ethyl alcohol. The most marked differences in efficiency have been found for specimens subjected to different cleaning treatments and annealed in the oxidizing atmosphere.

The characteristics shown in Figure 7 suggest that the specimens with a higher efficiency have, unfortunately, a longer decay time. For unannealed YAG:Ce plates, the decay time is 207 ns and the afterglow (1 μs after the end of the excitation) amounts to 12%. If the plates are cleaned in ethyl alcohol and then annealed in the oxidizing atmosphere, the decay time is shortened to 126 ns and the afterglow amounts to less than 7%. On the other hand, specimens which were boiled under the same conditions in aqua regia prior to their annealing

have a considerably slower cathodoluminescence with a decay time of 373 ns, and their afterglow reaches nearly 25%. The YAG:Ce single crystals which were annealed in the reducing atmosphere differ from the unannealed ones much less than the plates annealed in the oxidizing atmosphere. The specimens cleaned only in ethyl alcohol and annealed in H_2 have a decay time of 215 ns and their afterglow amounts to about 15%, whereas the specimens annealed under the same conditions but cleaned in advance by boiling in aqua regia have a decay time of 190 ns and the afterglow amounts to about 11%.

For all treatments of YAG:Ce single crystal, the degradation of efficiency was very low. The highest decrease of efficiency of the YAG:Ce single crystal has been found for unannealed specimens impacted by electrons with an energy of 10 keV and a current density of 4×10^{-8} A·cm^{-2}. During the first three hours, their efficiency decreased by about 3%. For specimens annealed in the reducing atmosphere, the efficiency forming did not exceed 2.5% under the same conditions, and for specimens annealed in the oxidizing atmosphere it amounted to about 1%. When the measurement was repeated later, the forming of efficiency started nearly at the original initial value, it was faster, and no additional degradation took place.

Proposals for applications

The YAG:Ce single crystals with a maximum attainable Ce concentration are unambiguously the most suitable crystals for any application in EM. As the activator concentration increases, the probability of trapping the excitation energy into defect centers decreases, which restricts the unfavorable effect of these defect centers. As a result, both the CL efficiency and the CL speed of the crystal increase. Therefore, it is very simple to decide about the magnitude of Ce concentration.

Deciding about the suitable way of cleaning and annealing of YAG:Ce single crystals is a bit more difficult. Methods that lead to a decrease in the decay time and particularly in the afterglow of YAG:Ce decrease the CL efficiency. And, vice versa, methods that lead to an increase in the CL efficiency, prolong the decay time and particularly the afterglow. The reason is that the way of cleaning and annealing has probably an effect on the support non-radiative transitions.

If the YAG:Ce single crystal is to be used as a scintillator for an electron detector in SEM/STEM, then the short decay time must be given preference over higher efficiency. For this purpose, the most suitable are YAG:Ce single crystals with Ce concentration higher than 3×10^{-1} mol% which must be annealed in an oxidizing atmosphere for at least 5 hours at 1500°C, after being shaped into a required geometry of a required size, but before depositing a thin conducting film. If,

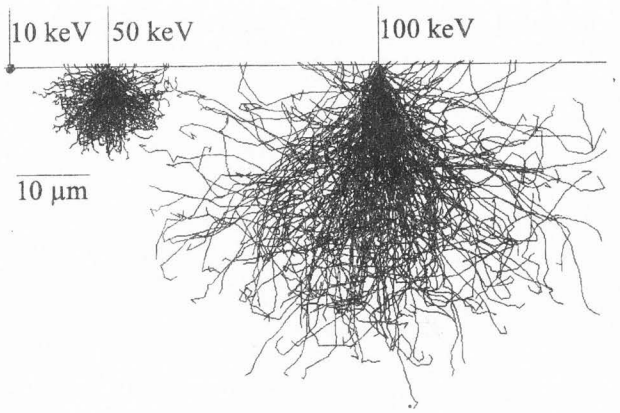

Figure 8. Monte Carlo trajectories of electrons in YAG for an impact electron energy of 10 keV, 50 keV and 100 keV. Two hundred and fifty trajectories were used for each energy.

---

however, the YAG:Ce single crystal is to be used as a CL screen in EM, where the demands on the CL speed are not so high, it is advantageous to use another treatment of the crystal with the maximum activator concentration. In that case, it is most suitable to anneal the YAG:Ce screen in the reducing atmosphere (H_2) under the same time and temperature conditions, prior to depositing a thin conducting layer.

Resolution of CL Screens

The size of interaction volumes in crystals, more exactly the surface projection of absorbed energy distribution, is an important CL property for the estimation of the resolution of images produced on screens by electrons with different energies. Therefore, the interaction volumes in CL single crystals for EM were simulated by the Monte Carlo (MC) method based on the plural large angle elastic scattering utilizing the screened Rutherford cross-section and Bethe's slowing down approximation (Love *et al.*, 1977; Joy, 1988). The MC model simulated 3-dimensional (3D) trajectories of primary electrons in the bulk of the investigated solid. Only primary processes were included in the model. In this work, attention was concentrated on the perpendicular impact of primary electrons but it is no problem to simulate also an inclined impact. Besides trajectories, also absorbed energy distribution was a result of MC simulation. The simulation program was written in Fortran 77 and it can be run on PC. Approximately 350 and 7000 trajectories per minute were calculated when imaging was allowed and forbidden, respectively, on the 486 DX2/66 MHz with the local bus.

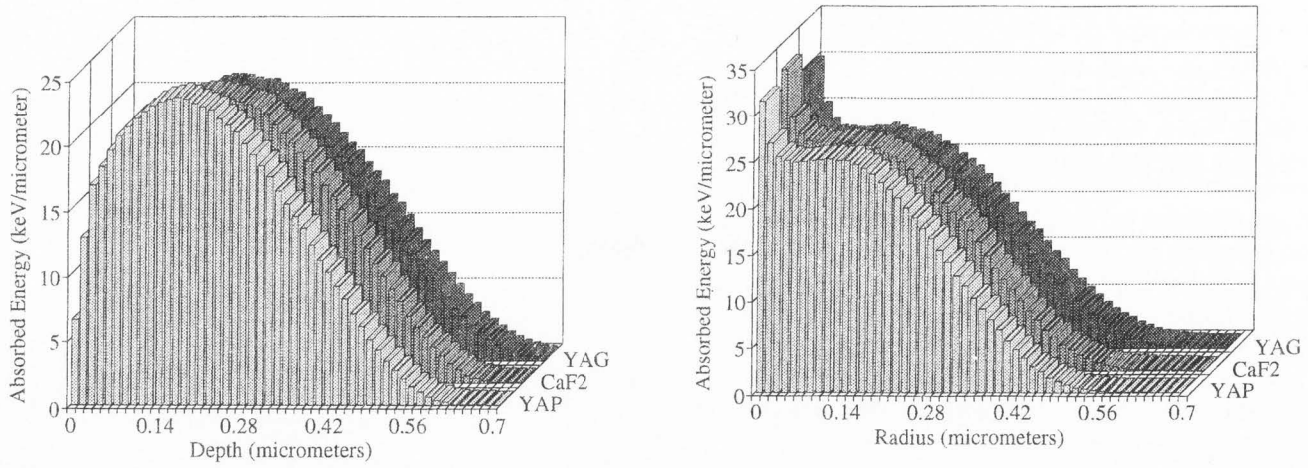

Figures 9 and 10. MC simulation of the longitudinal (in the direction of depth; **Fig. 9**) and transversal (in the direction of width; **Fig. 10**) distributions of the absorbed energy density. 10^5 trajectories and initial energy of 10 keV were used.

Interaction areas

The results of MC simulation of electron trajectories in YAG are given in Figure 8, which shows 3D trajectories projected into the plane perpendicular to the surface of material under investigation. The boundary between vacuum and the solid is indicated by the horizontal line, and the trajectories of primary beams with different energies (10 keV, 50 keV and 100 keV, respectively) are indicated by perpendicular lines above this horizontal boundary. The magnification is indicated by the scale line (10 μm). For the other single crystals investigated, the results are very similar.

It is obvious from Figure 8 that the electron interaction volume in YAG increases with increasing energy of incident primary electrons. From the viewpoint of CL properties of single crystals, this is a very important fact because at different energies a different part of the crystal determines the CL properties. At low energies ($<$ 10 keV), the CL properties are determined by the surface properties whereas at high energies ($>$ 100 keV) they are determined only by the volume properties of the single crystal. In other words, in the former case, abrasives, polish pastes, detergents, and the annealing used for the surface treatment, and in the case of very low energy incident electrons even the influence of the thin conducting layer, which must be deposited on the crystal surface, can play a very important role.

MC simulation of electron interaction volumes is of greater importance to CL screen resolution. However, one cannot make conclusions only on the basis of images of trajectories because the images do not carry sufficient information about the magnitude of energy absorbed in different parts of the trajectory, and, moreover, in these images it is not possible to distinguish places of repeated passages of electrons from places where only one passage takes place. And last, but not the least, three hundred trajectories, which is the highest possible number that still allows distinguishing of individual electron trajectories at high magnifications, is too low for obtaining statistically important results of the MC simulation method. As many as 10^3 or, better, 10^4 trajectories are necessary. However, if projected to obtain an image similar to that shown in Figure 8, so many trajectories would produce an entirely black semicircle that would hardly be of any use. Therefore, graphs of absorbed energy distribution are much more useful for CL screen resolution.

Distribution of absorbed energy

During each step of the motion of primary electrons, their energy losses are recorded. Separate recordings of the absorbed energy in the dependence on the depth (longitudinal distribution), and on the direction parallel to the surface (transversal distribution) were made. Figure 9 shows the longitudinal distribution of the absorbed energy density in YAG, CaF_2, and YAP single crystals for the perpendicular impact of 10^5 primary electrons with the 10 keV energy. This graph gives the amount of energy absorbed in the 1 μm thick layer at the given depth. From this figure it is possible to find the MC depth which is defined as an interaction depth which comprises 90% of the absorbed energy. MC depths calculated for YAG, CaF_2, and YAP at an impact electron energy of 10 keV are 0.46 μm, 0.43 μm and 0.40 μm, respectively.

Figure 10, which shows transversal energy density distribution, has been obtained by projecting the energy absorbed in the volume of material into the surface plane, for the same simulation input data as for Figure 9. The transversal energy density is defined as energy absorbed in the layer which is limited by two cylin-

ders having their axes on the line of electron incidence. The difference between their radii is 1 μm. In other words, it is the energy absorbed in the 1 μm annulus of the surface projection. As the transversal density must be distributed rotationally symmetrically around the point of incidence of an electron, it is possible to give transversal energy density distribution only in the dependence on the change in the radius from the centre of symmetry. From the figures showing transversal energy distribution it is possible to obtain information about the MC width (surface area diameter) which is defined as the width of the interaction volume comprising 90% of the absorbed energy. The MC width gives the first (rough) information about the CL area in bulk solids. Figure 10 shows MC simulation results of the transversal energy density distribution for the same single crystals and the same input data as those discussed for Figure 9. The MC widths calculated for YAG, CaF_2, and YAP at an impact electron energy of 10 keV result to 0.78 μm, 0.72 μm and 0.70 μm, respectively.

Energy dependence of interaction areas

As already mentioned above, the magnitudes of electron interaction areas in CL single crystals strongly depend on the energy of impact primary electrons. For YAG, this dependence is evaluated in Figure 11. The reason why YAG was chosen for the presentation of the obtained results is that it is most frequently used for CL screens in EM. However, the presented results are useful also for other single crystals investigated in this work because, as obvious from the MC simulation shown in Figures 9 and 10, the magnitudes of interaction areas for CaF_2 and YAP can be obtained by reducing the areas for YAG by about 10%. The graph in Figure 11, obtained by using the results of analytical and MC calculations, shows the energy dependence of the maximum and MC depths and widths. The maximum depths and widths (the theoretically attainable limit of the primary electrons penetration) have been calculated analytically using Bethe's formula. The MC depth and MC width are defined in the same way as in the previous chapter. The estimate of the dependence of the CL width, which was calculated using only the empirical formula (Garlick, 1966) is shown too.

It can be seen from Figure 11 that the MC width is smaller than double the MC depth because for the perpendicular impact of primary electrons the trajectories have more marked components in the direction perpendicular to the single crystal surface. For all simulated energies, the MC width corresponds approximately to the maximum depth, which is advantageous for a rough estimation of screen resolution made on the basis of an analytical evaluation. As MC simulation did not include electron diffusion, the CL width was determined by

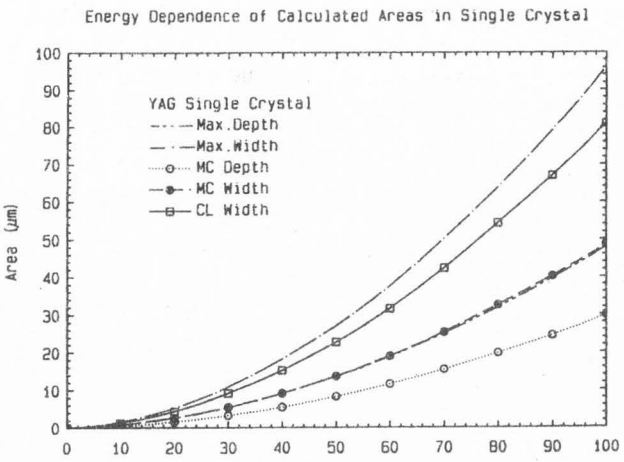

Figure 11. Dependence of the Bethe's depth and width, of the MC depth and width, and of the CL width on the energy of impact electron beam.

extending the MC width by means of empirical relations, and for YAG it amounts to 1.3 μm, 23 μm a 80 μm for electron energies 10 keV, 50 keV and 100 keV, respectively. For the 13 keV energy the results of CL width simulation (2 μm) are in agreement with the experimental results obtained by Sluzky and Hesse (1988). Using regression analysis, it can easily be found out that for YAG single crystals the characteristic of the increasing dependence of the CL width ϕ_{CL} on impact electron energy E has a form of power function (approx. $\phi_{CL} = 0.02E^{9/5}$ [μm; keV]). This is the essential difference between the single crystal screen and powder screen properties. For powder screens, the CL width is determined by the scattering of the emitted light which takes place on the individual grains of a non-compact phosphor rather than by the scattering of interacting electrons. It depends therefore on the magnitude of material grains and shows only a weak energy dependence (Valle *et al.*, 1984). For this reason, single crystal CL screens are more advantageous for lower electron excitation energies, because they provide higher resolution than powder screens. And, vice versa, for very high electron excitation energies, powder screens are more suitable because they are more capable of eliminating a large interaction volume when high energy primary electrons are absorbed, and so higher resolutions can be achieved.

Conclusion

The P47 single crystal seems to be the most suitable material for scintillators of electron detectors in SEM/STEM. It has the shortest decay time, no afterglow and a higher efficiency than other single crystal scintillators suitable for applications in EM. It is spectrally well matched to all alkaline photocathodes, so that

there are no problems regarding the choice of PMT. Its only but essential disadvantage is that it is available with difficulty because there are high demands on the crystal growth technology. On the other hand, yttrium aluminate single crystals (YAG:Ce and YAP:Ce) are commercially available, and, moreover, the latter crystal (technologically more demanding of the two) possesses properties that are only slightly worse than those of the P47 single crystal. However, if used in scintillation detectors in SEM/STEM, an increased attention must be paid to the choice of PMT and the light-guide because this scintillator emits light near the UV boundary of the optical spectrum.

The YAG:Ce single crystal remains probably the most frequently used CL material in EM. It is suitable both for use in scintillation detectors and as an imaging screen. If it is to be used as a scintillator, then preference must be given to its short decay time which means that it must be annealed in an oxidizing atmosphere, before being covered with a thin conducting film. Then for YAG scintillation detectors the use of PMT with a multialkali photocathode is recommended that has an extended sensitivity toward the red region of the spectrum. If the YAG:Ce single crystal is to be used as a CL screen, in which case the demands put on the CL speed are not severe, it is most suitable to anneal the screen in a reduction atmosphere. The CL resolution of YAG:Ce single crystal screens is primarily determined by the size of the electron interaction area, and for low excitation energies it is much lower than for classical powder screens. If submicron resolution is required, only YAG:Ce or other single crystal screens are applicable.

Acknowledgements

The authors wish to thank Dr. Jiří Kvapil, Dr. Josef Kvapil and Mr. K. Blažek from Preciosa Turnov for the cooperation during preparation of single crystal scintillators. They also thank Mrs. L. Pohanková for her assistance during compiling of this manuscript.

References

Arii T, Yoshimura N, Kamiya Y (1993) Intensity measurement of high-voltage electron-microscopic images by YAG-TV recording systems. J Electron Microsc **42**, 55-63.

Autrata R, Schauer P, Kvapil Jos, Kvapil Ji (1978) A single crystal of YAG:Ce - new fast scintillator in SEM. J Phys E: Sci Instrum **11**, 707-708.

Autrata R, Schauer P, Kvapil Ji, Kvapil Jos (1983) A single crystal of $YAlO_3:Ce^{3+}$ as a fast scintillator in SEM. Scanning **5**, 91-96.

Batson PE (1988) Parallel detection for high-resolution electron energy loss studies in the scanning transmission electron microscope. Rev Sci Instrum **59**, 1132-1138.

Delong A, Hladil K, Kolarik V (1994) A low voltage transmission electron microscope. Eur Microsc Anal No. 27, 13-15.

Dorenbos P, Visser R, Vaneijk CWE, Valbis J, Khaidukov NM (1992) Photon yields and decay times of cross luminescence in ionic crystals. IEEE Trans Nucl Sci **39**, 506-510.

Garlick GFJ (1966) Cathodo- and radioluminescence. In: Luminescence of Inorganic Solids. Goldberg P (ed.). Academic Press, New York. pp. 690-697.

Joy DC (1988) An introduction to Monte Carlo simulations. EUREM 88, Proc 9th Europ Cong Electron Microsc vol. 1. Inst. Physics, Bristol, UK. pp. 23-32.

Krivanek OL, Gubbens AJ, Dellby N (1991) Developments in EELS instrumentation for spectroscopy and imaging. Microsc Microanal Microstruct **2**, 315-332.

Kvapil Ji, Kvapil Jos, Manek B, Perner B, Autrata R, Schauer P (1981) Czochraski growth of YAG:Ce in reducing protective atmosphere. J Cryst Growth **52**, 542-545.

Kvapil Ji, Manek B, Perner B, Kvapil Jos, Becker R, Ringel G (1988) The role of argon in yttrium aluminates. Cryst Res Technol **23**, 549-554.

Lempicki A, Wojtowicz AJ, Berman E (1993) Fundamental limits of scintillator performance. Nucl Instrum Meth Phys Res **A333**, 304-311.

Love G, Cox MGC, Scott VD (1977) A simple Monte Carlo method for simulating electron-solid interactions and its application to electron probe microanalysis. J Phys D: Appl Phys **10**, 7-23.

Robbins DJ (1980) On predicting the maximum efficiency of phosphor systems excited by ionizing radiation. J Electrochem Soc **127**, 2694-2702.

Robbins DJ, Cockayne B, Lent B, Duckworth CN, Glasper JL (1979) Investigation of competitive recombination processes in rare-earth activated garnet phosphors. Phys Rev **B19**, 1254-1269.

Schauer P, Autrata R (1992a) Light transport in single-crystal scintillation detectors in SEM. Scanning **14**, 325-333.

Schauer P, Autrata R (1992b) Coatings of single crystal scintillators for electron detectors in SEM. EUREM 92, Proc 10th Europ Cong Electron Microsc vol. 1. pp. 107-108.

Sluzky E, Hesse K (1988) High-resolution phosphor screens. J Electrochem Soc **135**, 2893-2896.

Valle R, Genty B, Marraud A (1984) The effects of electron and light diffusion on the resolution of single crystal and conventional fluorescent screens. EUREM 84, Proc 8th Europ Cong Electron Microsc vol. 1. pp. 95-96.